Desalination and Water Treatment
www.deswater.com
20 (2010) 272–280
August
1944-3994 / 1944-3986 © 2010 Desalination Publications. All rights reserved.
doi: 10.5004/dwt.2010.1586

Equilibrium and kinetic studies of fluoride adsorption by chitosan coated perlite

Y. Vijaya, M. Venkata Subbaiah, A. Subba Reddy, A. Krishnaiah*

Biopolymers and Thermophysical Laboratories, Department of Chemistry, Sri Venkateswara University, Tirupati – 517 502, Andhra Pradesh, India
Tel. +91 9393621986; Fax: +91 877 2257614; email: abburikrishnaiah@gmail.com

Received 18 October 2009; Accepted in revised form 5 January 2010

ABSTRACT

A new biosorbent was developed by coating chitosan, a naturally and abundantly available biopolymer, on to perlite. The surface morphology of chitosan coated perlite (CCP) was observed using scanning electron microscopic (SEM) studies. Fourier transform infrared spectroscopy (FTIR) was used for the determination of functional groups responsible for fluoride sorption. The adsorption characteristics of CCP towards fluoride were studied under batch equilibrium and column flow experimental conditions. The effect of different process parameters such as pH, time, and concentration of fluoride and adsorbent dose on adsorption of fluoride was investigated. The data were analyzed on the basis of Lagergren first-order, pseudo-second-order and Weber–Morris models. The adsorption of fluoride on CCP followed pseudo-second-order kinetics. Break through curves were obtained from column flow adsorption data. The fluoride loaded CCP was regenerated using 0.1 N NaOH.

Keywords: Fluoride; Adsorption; CCP; Kinetics; Isotherms; SEM; FTIR

1. Introduction

Fluoride related health hazard is a major problem in many regions of the world. India is among the 25 nations around the globe where health problems occur due to the consumption of fluoride contaminated water. Fluoride is a necessary micronutrient both for human beings and animals. More than 60% of our fluoride demand is fulfilled by the consumption of drinking water. Thus fluoride present in the drinking water can have beneficial or detrimental effect depending on its concentration and consumption of total amount [1]. Excess of fluoride (> 1.5 mg/L) in drinking water is harmful to the human health [2]. According to the World Health Organization (WHO) the maximum acceptable concentration of fluoride in drinking water lies below 1.5 mg/L [3]. Fluoride is attracted by positively charged calcium in teeth and bones due to its strong electro negativity, which results in dental, skeletal, and non skeletal forms of fluorosis, in children as well as adults [4]. Fluoride normally enters the environment and human body through water, food, industrial exposure, drugs, cosmetics, etc. However, drinking water is the single major source of daily intake. Increasing fluoride concentration in water has already become a very serious issue in many countries [5]. The physiological effects of fluoride upon human health have been studied since early part of 20th century. Several reports and studies [6] established both the risk of high fluoride dosing and the benefits of minimal exposure [7]. A low dose of fluoride was deemed responsible for

* Corresponding author.

inhibiting dental carries while a higher daily dose was linked to permanent tooth and skeletal fluorosis [8].

Various treatment technologies, based on the principle of precipitation, ion exchange, electrolysis, membrane and adsorption process were used for removal of fluoride from drinking water as well as industrial effluents [9]. Removal of fluoride was studied by adsorption on activated alumina [10], alum [11], charcoal [12], waste mud [13], chitosan [14,15], ion exchange [16], electrocoagulation [17] and membrane process such as reverse osmosis, nanofiltration, electro dialysis and donnan dialysis [18–20].

Chitosan is a hydrophilic, natural cationic polymer formed by the *N*-deacetylation of chitin, which is present in fungi, insects, and crustaceans [21]. It is an effective ion-exchanger, with a large number of amino groups. The presence of these amino groups increases the adsorption capacity of chitosan compared to that of chitin, which only has a small percentage of amino groups [22]. Recently, Ma et al. [23] studied adsorption of fluoride on magnetic-chitosan particle from the water solution in the batch system. Perlite is used to a limited extent as an adsorbent for methylene blue [24] and as solid support in chromatography [25,26]. In the present investigation, the expanded form of perlite is used as a substrate for the preparation of beads. The adsorption capacity can be enhanced by spreading chitosan on physical supports that can increase the accessibility of the adsorbate-binding sites [27].

The primary objective of this research was to study the biosorption of fluoride from aqueous medium by CCP beads under equilibrium and column flow conditions. The secondary objective was to investigate the effect of pH, contact time, concentration of fluoride and amount of biomass on the extent of adsorption. The tertiary objective included the fitting of the experimental data to adsorption isotherms, Lagergren first-order, pseudo second-order and Weber–Morris intraparticle diffusion kinetic models.

2. Material and methods

2.1. Chemicals

Sodium fluoride (NaF), sodium chloride (NaCl), sodium hydroxide (NaOH), acetic acid (CH_3COOH), hydrochloric acid (HCl) and oxalic acid ($H_2C_2O_4$) were obtained from Sd. Fine Chem. Pvt. Ltd. India. Total ionic strength adjustable buffer (TISAB), used to eliminate other interferences in fluoride solution, purchased from Thermo Electron Corporation, USA. Chitosan, having an average molecular weight of 300,000 was purchased from Aldrich Chemical Corporation, USA. Perlite was obtained from Silbrico Corporation, IL, USA. Stock solution of fluoride was prepared by dissolving 2.21 g of NaF in 1000 ml of double distilled water. The stock solution was then appropriately diluted to get the test solution of desired fluoride concentrations.

2.2. Preparation of chitosan coated perlite beads

Perlite was first mixed with 0.2 M oxalic acid and the mixture was stirred for 12 h at room temperature and filtered. The filtered perlite was washed with deionized water and dried overnight at 70°C, and sieved through 100-mesh size. The acid treated perlite was stored in desiccator. About 30 g of medium molecular weight chitosan was slowly added to 1 L of 0.2 M oxalic acid solution under continuous stirring at 40–50°C to facilitate the formation of viscous gel. About 60 g of acid treated perlite powder was mixed with deionized water and slowly added to the diluted gel and stirred for 12 h at 40–50°C. The highly porous beads were then prepared by drop wise addition of perlite gel mixture into a 1M NaOH precipitation bath. The purpose of adding acidic perlite–chitosan mixture to NaOH solution was to assist rapid neutralization of oxalic acid, so that the spherical shape could be retained. The beads were separated from NaOH bath, and washed several times with deionized distilled water to a neutral pH. The beads were dried in a freeze drier, oven and by air.

2.3. Batch equilibrium studies

In order to explore the effect of influencing factors, such as pH, contact time, quantity of adsorbent and the initial concentrations of fluoride solution, a series of batch experiments were conducted. The stock solutions were diluted to required concentrations (5, 10, 15, 20 and 25 mg/L). Batch adsorption experiments were performed by agitating specified amount of adsorbent in 100 ml of fluoride solutions of desired concentrations at varying pH in 125 ml stopper bottles. The pH of the suspension was adjusted with 0.1 N HCl and 0.1 N NaOH. The mixture was agitated at 200 rpm for a known period of time at room temperature in a mechanical shaker. After equilibrium, the aqueous-phase concentration of fluoride was analyzed with Orion ion selective electrode (I.S.E). Adsorption of fluoride on the glassware was found to be negligible and was determined by running blank experiments. The percentage removal of fluoride was obtained using the equation:

$$\%\,\text{removal} = \frac{(C_o - C_e)}{C_o} \times 100 \quad (1)$$

The amount adsorbed per unit mass of adsorbent at equilibrium q_e (mg/g) was obtained using the equation.

$$q_e = \left(\frac{C_o - C_e}{m}\right) v \quad (2)$$

where C_o and C_e denote the initial and equilibrium fluoride concentrations (mg/L) respectively; v is the volume of the solution in liters, and m is the mass of the adsorbent used (g).

2.4. Column adsorption experiments

Column studies were carried out in a column made of Pyrex glass of 1.5 cm internal diameter and 10 cm length. The column was filled with 3 g of dried CCP beads by tapping so that maximum amount of adsorbent was packed without gaps. The influent aqueous fluoride solution containing known concentration was filled in the reservoir of large cross sectional area so that the change in the height of the liquid level was negligible during the experiment. Due to the negligible change in the height of the liquid level the flow rate remains constant. The influent solution was allowed to pass through the bed at constant flow rate of 2 ml/min, in down flow manner with the help of a fine metering valve. All the experiments were carried out at room temperature. The effluent solution was collected at different time intervals and the concentration of the fluoride in the effluent solution was monitored by Orion 4 star series meter.

2.5. Column desorption studies

Desorption (regeneration) studies are very important since the success of adsorption process depends on the regeneration of adsorbent. There are several methods for the desorption of the adsorbate from the loaded adsorbents. In the present study the elution method with solvent is used to remove the adsorbed fluoride from CCP beads.

After the column was exhausted, the column was drained off the remaining aqueous solution by pumping air. Desorption of solutes from loaded adsorbent were carried out by solvent elution method using 0.1 N NaOH as an eluent. The NaOH solution was pumped into the column maintained at constant temperature at a fixed flow rate (2 ml/min). From the start of the experiment effluent samples at different intervals, are collected at the bottom of the column for analysis. After the regeneration, the adsorbent column is washed with distilled water to remove NaOH from the column before the influent fluoride solution is reintroduced for the subsequent adsorption–desorption cycles. Adsorption–desorption cycles were performed thrice for fluoride using the same bed to check the sustainability of the bed for repeated use.

3. Results and discussion

3.1. Characterization of CCP beads

3.1.1. Fourier transform infrared (FTIR) studies

The FTIR spectrum of CCP beads is shown in Fig. 1a. The broad band in the region between 3010–3000 cm^{-1} is due to the overlapping of the stretching frequencies of –OH and $–NH_2$ groups. The bands at 2922.1 cm^{-1} and 1428.1 cm^{-1} represent stretching and bending frequencies of $–CH_2$ groups. The bands at 1642.3 cm^{-1} and 1072.9 cm^{-1} are observed due to the bending and stretching of $–NH_2$ and –COO– groups, respectively. The presence of –C–O and –C–N linkages is confirmed from the peaks at 1316.4 cm^{-1} and 1021.5 cm^{-1}. The FTIR spectra of CCP loaded with fluoride is given in Fig 1b. In the spectrum a new band is observed at 1010 cm^{-1}, which can be assigned to –C–F bonding. Further, the figure indicate that there is a shift in absorption frequency of amino and hydroxyl groups, which signify the deformation of –OH, –COO–, –NH bonds. These may be attributed to the interaction

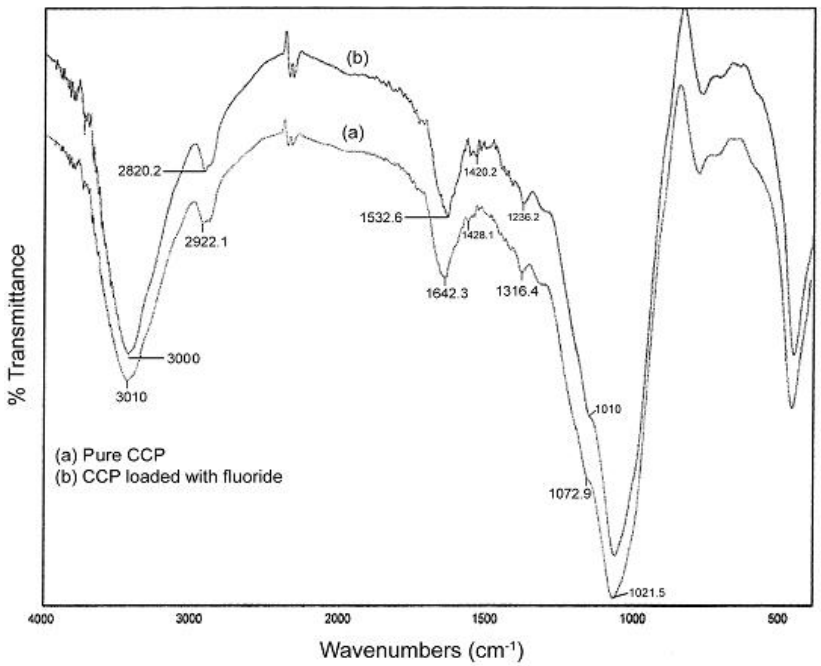

Fig. 1. FTIR spectra of (a) CCP and (b) CCP loaded with fluoride.

between the functional groups of CCP with fluoride during the adsorption process. These results confirm the participation of amino and hydroxyl groups of CCP beads as potential active binding sites for adsorption of fluoride.

3.1.2. Surface area analysis

Surface area, density, pore volume, pore diameter and porosity of the composite biosorbent were determined with BET and pycnomatic ATC instruments. Surface area was measured by assuming that the adsorbed nitrogen forms a monolayer and posses a molecular cross sectional area of 16.2 A°. The isotherm plots were used to calculate the specific surface area (N_2/BET method) and average pore diameter of CCP beads, while micro pore volume was calculated from the volume of nitrogen adsorbed at p/p_0 1.4. The sorbent material shows an average surface area of 112.3 $m^2\ g^{-1}$ and pore volume of 0.47 $cm^{-3}\ g^{-1}$. The surface characteristics of CCP beads are summarized in Table 1.

3.1.3. Scanning electron microscopic (SEM) studies

Scanning electron micrograph (SEM), recorded using a soft ware controlled digital scanning electron microscope, are given in Fig. 2. The SEM of the samples was taken to study the surface morphology. The SEM of pure perlite powder showed no particular shape or crystalline structure and it rather appeared like flakes Fig. 2a. The surface morphology of the perlite appears to change significantly following coating with chitosan. The SEM micrograph of the outer surface of CCP beads is shown in Fig. 2b. The average size of particles is 100–150 μ and that the shape of composite particle can be described as spherical. The figure also illustrates the surface texture and porosity of CCP beads with holes and small openings on the surface, thereby increasing the contact area, which facilitates the pore diffusion during adsorption. The beads are cut into half and then the SEM of the internal surface is recoded and included in Fig. 2c. The porous nature is clearly evident from this micrograph. The surface morphology and texture of coated perlite are completely different compared to uncoated perlite. The inner surface appears to have similar type of texture and morphology as the outer surface.

Table 1
Surface properties of CCP

S. No.	Property	Chitosan coated perlite
1	Surface area, $m^2\ g^{-1}$	112.25
2	Porosity, %	43.41
3	Pore volume, $cm^3\ g^{-1}$	0.47
4	Pore diameter, cm g^{-1}	0.97
5	Density, g cm^{-3}	3.13
6	Ion exchange capacity, meq g^{-1}	0.92

3.2. Effect of pH

The pH of the aqueous solution is a controlling factor in the adsorption process. Thus the role of hydrogen ion concentration was examined at pH values 2–10. The pH was adjusted by adding 0.1 N HCl or 0.1 N NaOH with 100 ml of 5, 10, 15, 20 and 25 mg/L of fluoride solution for a contact time of 120 min with a dose of 0.5 g of adsorbent. Chloride is not influence to adsorb fluoride using CCP. The influence of pH for the removal of fluoride is shown in Fig. 3. We have observed increase in the extent of removal of fluoride with increase in the pH of the solution. This was investigated as maximum removal of fluoride was observed 52, 64, 70, 75 and 78 % for 5, 10, 15, 20 and 25 mg/L at pH 6. Above pH 6 the % removal of fluoride decreases slowly due to the formation of precipitation of hydroxides [28] of metal ions present in perlite as aluminium hydroxide and magnesium hydroxide.

3.3. Equilibrium modeling

The experimental data are fitted to the Langmuir isotherm [29] of the form:

$$Q_e = \frac{Q^o b C_e}{1 + b C_e} \tag{3}$$

where Q_e is the amount of fluoride adsorbed (mg/g), C_e is the equilibrium concentration of fluoride ion (mg/L), Q^o is the amount of adsorbate at complete monolayer coverage (mg/g), which gives the maximum sorption capacity of

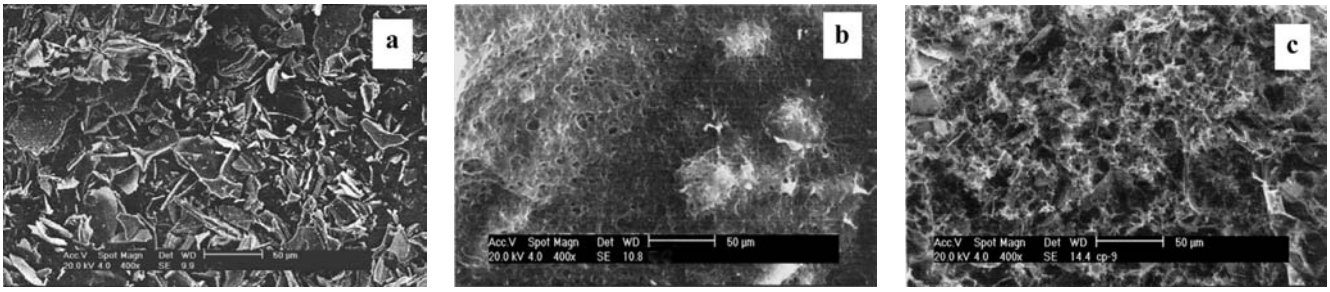

Fig. 2. SEM images of (a) pure perlite powder, (b) outer surface of CCP and (c) cross section of CCP.

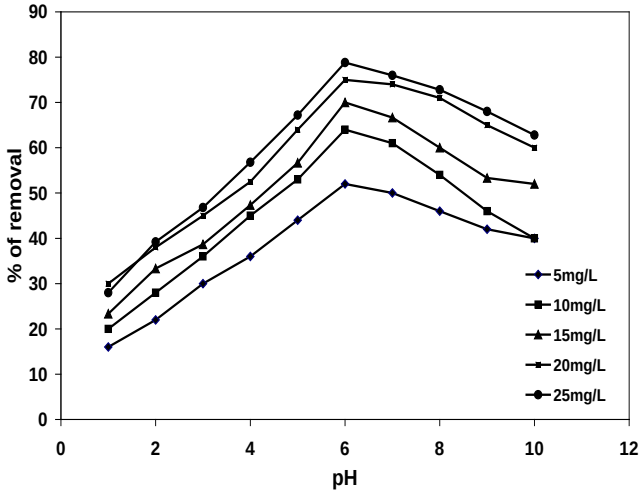

Fig. 3. Effect of pH on biosorption of fluoride on CCP.

the sorbent, b (L/mg), is the Langmuir isotherm constant that relates to the energy of adsorption.

In order to find out the feasibility of the isotherm, the essential characteristics of the Langmuir isotherm can be expressed in terms of a dimensionless constant, separation factor or equilibrium parameter, R_L [30]:

$$R_L = \frac{1}{1 + bC_o} \tag{4}$$

where C_o and b are the initial concentration of fluoride and Langmuir isotherm constant. The value of $R_L < 1.0$ represent favorable adsorption and greater than 1.0 represent unfavorable adsorption. The values of R_L for sorption of fluoride on CCP are less than 1 and greater than 0, indicating the favorable uptake of fluoride by the CCP.

The equilibrium data are also fitted Freundlich [31] equation, which takes the form:

$$Q_e = K_f C_e^{1/n} \tag{5}$$

where Q_e is the amount of fluoride adsorbed per unit weight of the sorbent (mg/g), C_e is the equilibrium concentration of fluoride ion solution (mg/L), K_f is a measure of adsorption capacity, and $1/n$ is the adsorption intensity. The values of Langmuir constants Q^o and b and Freundlich parameters K_f, $1/n$ and n along with the correlation coefficient (r^2) are presented in Table 2. Among these two models, the experimental data are well-fitted to the Langmuir model compared to Freundlich model due to the value of correlation coefficient r^2 for the Langmuir model is relatively high as shown in Table 2. Values of $1/n$ are lying between 0.1 and 1.0 confirms the favorable conditions for adsorption.

Dubinin–Radushkevich (D–R) equation has been widely used to explain energetic heterogeneity of solid surface at the monolayer region in micro-pores [32]. In order to better understand and clarify the adsorption process, equilibrium data were evaluated by D–R isotherm.

Table 2
Langmuir, Freundlich and Dubinin isotherm constants for adsorption of fluoride on CCP

Isotherm model	Parameter			
Langmuir	Q^o	b	r^2	
	64.1	0.003	0.996	
Freundlich	K_f	n	$1/n$	r^2
	4.141	1.070	0.934	0.989
Dubinin–Radushkevich	K	ln Q^o	E	r^2
	0.002	3.006	16.22	0.989

$$Q = Q_m \exp\left(-k\varepsilon^2\right) \tag{6}$$

and linearized form of the equation is given as

$$\ln Q = \ln Q_m - k\varepsilon^2 \tag{7}$$

where ε (Polanyi potential) is [RT ln (1+ (1/C_e)], Q is the amount of fluoride adsorbed per unit weight of adsorbent (mol/g), k is a constant related to the adsorption energy (mol^2 kJ) and Qm is the adsorption capacity (mol/g), where R (Jmol^{-1}K^{-1}) is the gas constant; and T (K), the absolute temperature.

The mean free energy of adsorption (E), defined as the free energy change when 1 mol of ion is transferred to the surface of the solid from infinity in solution can be calculated from the K value using the equation:

$$E = (-2K)^{-0.5} \tag{8}$$

The magnitude of E is useful for estimating the type of adsorption process. The mean free energy of adsorption E, gives information about adsorption mechanism as chemical ion-exchange or physical adsorption. The magnitude of E above 8 kJ/mol, the adsorption process follows chemical ion-exchange while for the values of $E <$ 8 kJ/mol, the adsorption process is of a physical nature. The mean adsorption energy (E) was calculated as 16.22 kJ/mol (Table 2) for the adsorption of fluoride on to CCP beads indicating that the adsorption of fluoride on to CCP beads proceeds via chemical ion-exchange mechanism.

3.4. Effect of contact time

Fig. 4 shows the effect of contact time on the extent of adsorption of fluoride on CCP beads (at five initial fluoride concentrations). It has been observed that maximum adsorption takes place during 120 min. The data obtained from this experiment were further used successfully to evaluate the kinetics of the adsorption process.

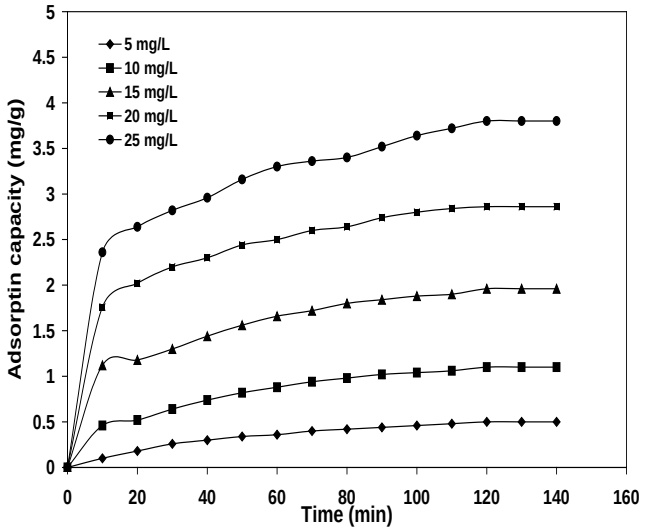

Fig. 4. Effect of time on biosorption of fluoride on CCP.

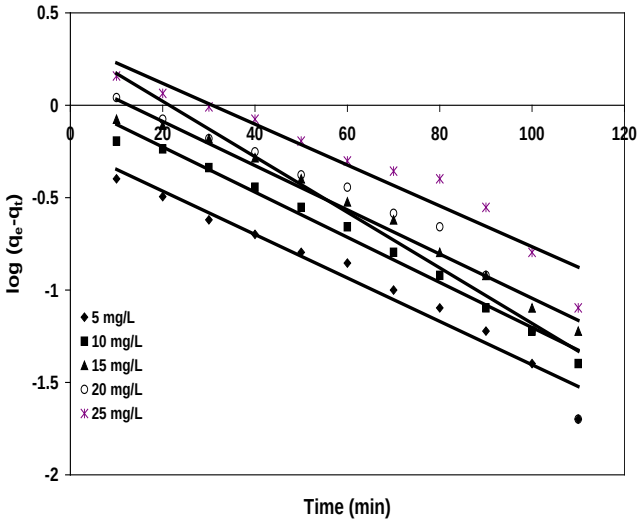

Fig. 5. Lagergren first-order kinetic plots for biosorption of fluoride on CCP.

3.4.1. Kinetic studies

Adsorption of fluoride was rapid for the first 60 min and its rate gradually slowed down as the equilibrium approached. The rate constant K_{ad} for sorption of fluoride was studied by Lagergren first-order rate equation [33].

$$\log(q_e - q_t) = \log q_e - \left(\frac{K_{ad}}{2.303}\right)t \quad (9)$$

Straight line plots of log $(q_e - q_t)$ vs. t at different times indicate the validity of Lagergren rate equation. The plots of log $(q_e - q_t)$ vs. t were straight line with $r^2 > 0.98$, indicates the validity of Lagergren equation of first order kinetics (Fig. 5). The adsorption rate constant (K_{ad}), calculated from the slope of the plot was found to be 0.027, 0.028, 0.028, 0.029, and 0.025 min^{-1} for initial concentrations of 5, 10, 15, 20, and 25 mg/L under experimental conditions (Table 3).

The pseudo-second-order kinetic model [34] in its integrated and linearized form has been used.

$$\frac{t}{q_t} = \frac{1}{K_2 q_e^2} + \frac{1}{q_e}t \quad (10)$$

where $K_{2,\,ads}$ (g mg min^{-1}) is the rate constant of second-order adsorption. The plot t/q_t vs. t giving a straight line (Fig. 6) showed second-order kinetics applicable and q_e and K_2 were determined from the slope and intercept of the plot, respectively.

Table 3 lists the results of rate constant studies for different initial fluoride concentrations by the pseudo-second-order model. The value of correlation coefficient r^2 for the pseudo-second-order adsorption model is relatively high (> 0.993), and the adsorption capacities calculated by the model are also close to those determined by experiments. Therefore it has been concluded that the pseudo-second-order adsorption model is more suitable to describe the adsorption kinetics of fluoride over CCP beads.

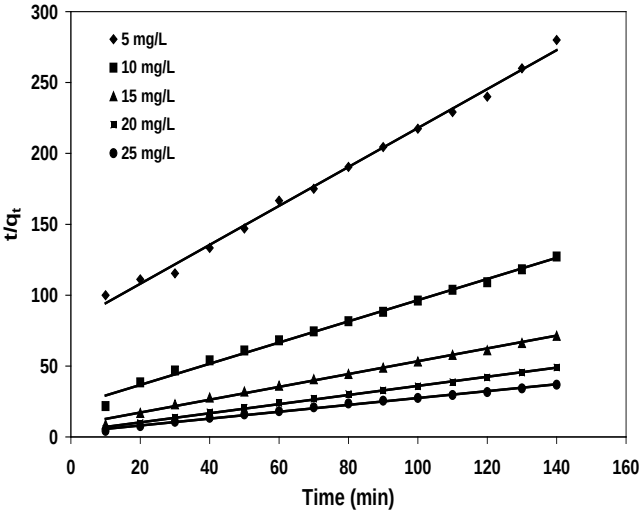

Fig. 6. Pseudo second-order kinetic plots for biosorption of fluoride on CCP.

3.4.2. Intra particle diffusion (Weber–Morris) model

The pore (intraparticle) diffusion model used here refers to the theory proposed by Weber and Morris [35]. If the rate limiting step is intraparticle diffusion, a plot of solute sorbed against square root of contact time should yield a straight line passing through the origin [36]. The intraparticle diffusion equation is:

$$q_t = K_{id} t^{1/2} \quad (11)$$

Table 3
Kinetic parameters for fluoride biosorption on CCP

Concentration of fluoride solution (mg/L)	First-order model		Second-order model				Intraparticle diffusion model		
	K_{ad}	r^2	$Q_{e\,exp.}$ (mg/g)	$Q_{e\,cal.}$ (mg/g)	K_2	r^2	K_{id}	C	r^2
5	0.027	0.965	0.50	0.75	0.022	0.995	0.046	0.005	0.984
10	0.028	0.986	1.10	1.34	0.025	0.993	0.091	0.122	0.966
15	0.028	0.982	1.96	2.21	0.025	0.995	0.146	0.422	0.905
20	0.029	0.948	2.86	3.11	0.027	0.998	0.200	0.816	0.834
25	0.025	0.932	3.80	4.13	0.020	0.995	0.264	1.046	0.845

where K_{id} is the intraparticle diffusion rate constant (mg/g. $min^{1/2}$). The plots are shown in Fig. 7 for the system investigated. The slope of the plot of q_t against $t^{1/2}$ will give the value of the intraparticle diffusion coefficient as shown in Table 3. It can be seen that all plots have an initial curved portion, followed by a linear portion. The initial curve of the plot is due to the diffusion of fluoride through the solution to the external surface of CCP or the boundary layer diffusion.

3.5. Effect of adsorbent dose

The effect of adsorbent dose on the removal of fluoride at optimum pH (6) is shown in Fig. 8. The amount of adsorbent significantly influences the extent of fluoride adsorption. The extent of maximum fluoride removal was 60, 65, 72, 75 and 78% for 5, 10, 15, 20 and 25 mg/L with 0.7 g of biosorbent. This increase in loading capacity is due to the availability of higher number of fluoride ions per unit mass of adsorbent, i.e. higher fluoride/adsorbent ratio. It can also be seen that the fluoride removal markedly increased up to adsorbent dose of 0.7 g due to increase in adsorbent/fluoride ratio however further increase in adsorbent dose does not show any appreciable improvement in fluoride removal.

3.6. Column adsorption and desorption studies

Column adsorption studies of fluoride on CCP beads at room temperature are investigated using aqueous solution of 25 mg/L influent concentration (C_o), at optimum pH value. Experimental breakthrough curves are obtained by plotting a graph between the ratio of effluent (C_e/C_o) against volume of solution and shown in Fig. 9. The data is obtained by passing the fluoride solution through a bed with 3 g of CCP beads in a downward flow of 2 ml/min and determining the concentration of fluoride at different time intervals in the effluent solution. When the column gets saturated, it is generated and subsequently used for next adsorption process. The adsorption– desorption cycles are repeated thrice. It is observed the

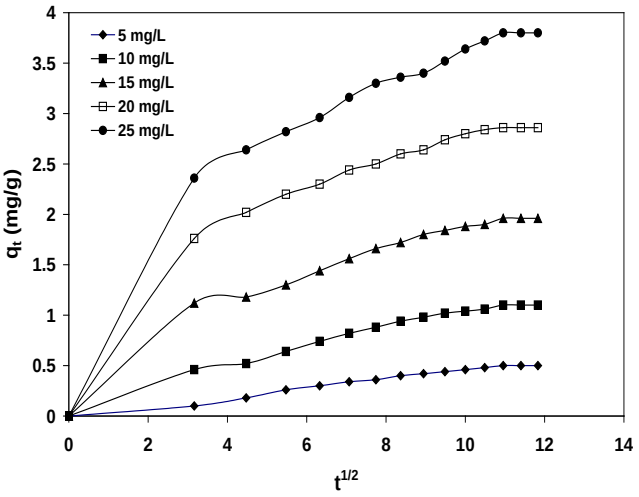

Fig. 7. Weber–Morris model for biosorption of fluoride on CCP.

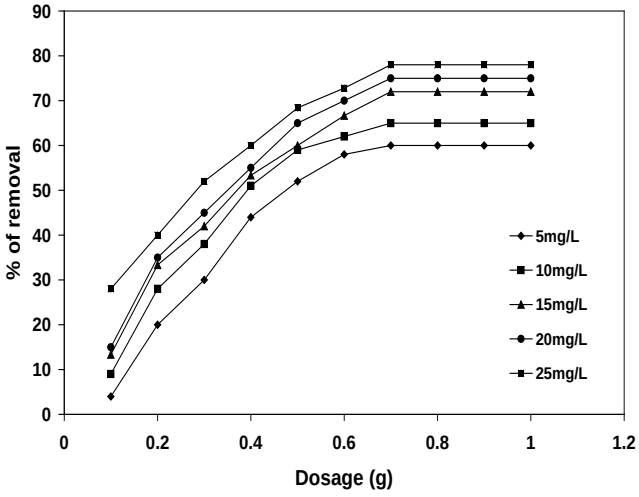

Fig. 8. Effect of adsorbent dose on percent removal of fluoride on CCP.

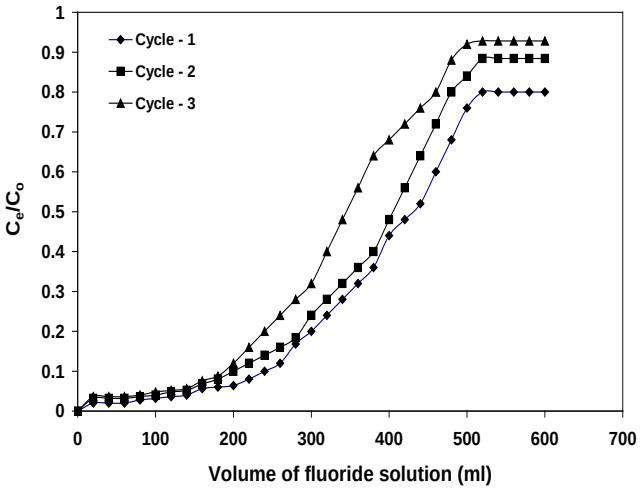

Fig. 9. Column breakthrough curves for adsorption of fluoride on CCP.

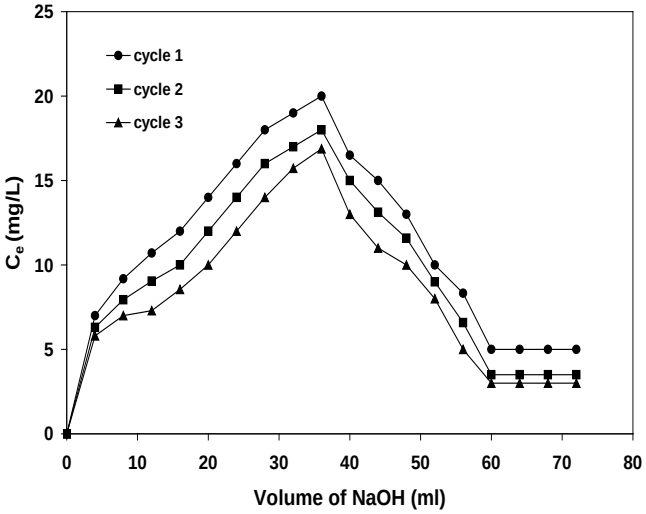

Fig. 10. Desorption curves of fluoride adsorbed on CCP.

column gets saturated after passing of 520 ml of fluoride solution in the first cycle. From the graph it gives the effective binding capacity of the biosorbent in each cycle. From the data it can be concluded that CCP is a good biosorbent for the removal of fluoride.

The regeneration could be accomplished by a variety of techniques such as thermal desorption, steam washing, solvent extraction etc. Each method has inherent advantages and limitations. In this study several solvents are tried to regenerate the adsorption bed. 0.1 M NaOH solution is found to be effective in desorbing and removing fluoride ion quantitatively from the adsorbent bed. The fixed bed columns of CCP beads saturated with fluoride solution is regenerated by passing 0.1 N NaOH solution as an eluent at fixed flow rate of 2 ml/min. More specifically maximum desorption 80, 86 and 88% occurs at 60 ml of 0.1 N NaOH solutions at 30 min for cycle 1, 2 and 3 respectively. It is observed that there is an early saturation of the bed with fluoride in 2nd and 3rd cycles. The desorption is graphically presented in Fig. 10. From the plots it is observed that the rate of desorption increases sharply reaching maximum with about 60 ml of 0.1 N NaOH solution.

4. Conclusions

Through the present study, it is demonstrates that a biobased sorbent was developed by coating chitosan on to perlite and the sorbent could be used successfully for the removal of fluoride from water. The sorbent is characterized on the basis of surface morphology, SEM and FTIR spectral techniques. The adsorption characteristics of the sorbent for fluoride ion are investigated under batch equilibrium and column flow experimental conditions. The equilibrium adsorption data are correlated by Langmuir, Freundlich and Dubinin–Radushkevich isotherm equations. The kinetic studies indicate that the sorption of fluoride on CCP follows pseudo-second-order kinetics. This model seems to be better fit than the other two models (pseudo first order and particle diffusion models) for representing the kinetics of fluoride sorption. The maximum biosorption capacity of CCP used in this study is 64.1 mg/g. Breakthrough curves for adsorption of fluoride on the sorbent were obtained using column flow experimental data.

References

[1] E.J. Underwood, Trace Elements in Human and Animal Nutrition, Academic Press, New York, 1997, 545 p.
[2] WHO (World Health Organization), Fluorine and Fluorides, Environmental Health Criteria, Geneva, 1984.
[3] S. Ayoob and A.K. Gupta, Fluoride in drinking water: A review on the status and stress effects, Environ. Sci. Technol., 36 (2006) 433–487.
[4] A.K. Susheela, A. Kumar, M. Betnagar and M. Bahadur, Fluoride in water: A UK perspective, Fluoride, 26 (1993) 97–104.
[5] S. Meenakshi and R.C. Maheswari, Fluoride in drinking water and its removal, J. Hazard. Mater., 137 (2006) 456–463.
[6] M. Hichour, F. Persin, J. Sandeaux and C. Gavach, Fluoride removal from waters by Donnan dialysis, Separ. Purif. Technol., 18 (2000) 1–11.
[7] A.K. Susheela, Treatise on Fluorosis, Fluorosis Research and Rural Development Foundation, India, 2001.
[8] M. Mahramanlioglu, I. Kizilcikli and I.O. Bicer, Adsorption of fluoride from aqueous solution by acid treated spent bleaching earth, J. Fluorine Chem., 115 (2002) 41–47.
[9] T. Tuiz, F. Persin, M. Hichour and J. Sandeaux, Modelisation of fluoride removal in Donnan dialysis, J. Membr. Sci., 212 (2003) 113–121.
[10] G.J. Fink and F.K. Lindsay, Activated alumina for removing fluorides from drinking water, Ind. Eng. Chem., 28(8) (1936) 947–948.
[11] K.R. Bulusu and W.G. Nawlakhe, Defluoridation of water with activated alumina continuous con-tacfing system, Ind. J. Environ. Health, 32(2) (1990) 197–218.

[12] W. Rongshu, L. Haiming, N. Ping and W. Ying, Study of a new adsorbent for fluoride removal from waters, Water Qual. Res. J. Can., 30(1) (1995) 81–88.
[13] B. Kemer, D. Ozdes, A. Gundogdu, V. Bullet, C. Duran and M. Soylak, Removal of fluoride ions from aqueous solution by waste mud, J. Hazard. Mater., 168 (2009) 884–894.
[14] C.S. Sundaram, N. Viswanathan and S. Meenakshi, Uptake of fluoride by nano-hydroxyapatite/chitosan, a bioinorganic composite, Bioresource Technol., 99 (2008) 8226–8230.
[15] N. Viswanathan, C.S. Sundaram and S. Meenakshi, Development of multifunctional chitosan beads for fluoride removal, J. Hazard. Mater., 167 (2009) 325–331.
[16] A.S. Behrman and H. Gustafson, Removal of fluorine from water: A development in the use of tricalcium phosphate, Ind. Eng. Chem., 30(9) (1938) 1011–1113.
[17] N. Drouiche, H. Lounici, M. Drouiche, N. Mameri and N. Ghaffour, Removal of fluoride from photovoltaic wastewater by electrocoagulation and products characteristics, Desal. Wat. Treat., 7 (2009) 236–241.
[18] R. Simons, Trace element removal from ash dam waters by nanofiltration and diffusion dialysis, Desalination, 89 (1993) 325–341.
[19] S.K. Adhikary, U.K. Tipnis, W.P. Harkare and K.P. Govindan, Defluoridation during desalination of brackish water by electrodialysis, Desalination, 71 (1981) 301–312.
[20] T. Ruiz, F. Persin, M. Hichour and J. Sandeaux, Modelisation of fluoride removal in Donnan dialysis, J. Memr. Sci., 212 (2003) 113–121.
[21] G. Rojas, J. Silva, J.A. Flores, A. Rodriguez, M. Ly and H. Maldonado, Adsorption of chromium onto cross-linked chitosan, Separ. Purif. Technol., 44 (2005) 31–36.
[22] S.P. Camble, S. Jagtap, N.K. Labsetwar, D. Thakare, S. Godfrey, S. Devotta and S.S. Rayalu, Defluoridation of drinking water using chitin, chitosan and lanthanum-modified chitosan, Chem. Eng. J., 129 (2007) 173–180.
[23] W. Ma, F.Q. Ya, M. Han and R. Wang, Characteristics of equilibrium, kinetics studies for adsorption of fluoride on magnetic-chitosan particle, J. Hazard. Mater., 143 (2007) 296–302.
[24] D. Mehmet, A. Mahir and O. Yavuz, Adsorption of methylene blue from aqueous solution onto perlite, Water. Air. Soil. Pollut., 120 (2000) 229–235.
[25] S. Kalyani, J. Ajitha Priya, P. Srinivasa Rao and A. Krishnaiah, Removal of copper and nickel from aqueous solutions using chitosan coated on perlite as biosorbent, Separ. Sci. Technol., 40 (2005) 1483–1495.
[26] S. Hasan, A. Krishnaiah, T.K. Ghosh, D.S. Viswanath, V.M. Boddu and E.D. Smith, Adsorption of divalent cadmium (Cd(II)) from aqueous solutions onto chitosan-coated perlite beads, Ind. Eng. Chem. Res., 45 (2006) 5066–5077.
[27] E. Guibal, C. Milot and J.M. Tobin, Metal-anion sorption by chitosan beads: Equilibrium and kinetic studies, Ind. Eng. Chem. Res., 37 (1998) 1454–1463.
[28] E. Oguz, Adsorption of fluoride on gas concrete materials, J. Hazard. Mater., 117 (2005) 227–233.
[29] D.A. Fungaro, M. Bruno and L.C. Grosche, Adsorption and kinetic studies of methylene blue on zeolite synthesized from fly ash, Desal. Wat. Treat., 2 (2009) 231–239.
[30] W. Zheng, X.M. Li, Q. Yang, G.M. Zeng, X.X. Shen, Y. Zhang and J.J. Liu, Adsorption of Cd(II) and Cu(II) from aqueous solution by carbonate hydroxylapatite derived from eggshell waste, J. Hazard. Mater., 147 (2007) 534–539.
[31] M.M. Abd El-Latif and A.M. Ibrahim, Adsorption, kinetic and equilibrium studies on removal of basic dye from aqueous solutions using hydrolyzed oak sawdust, Desal. Wat. Treat., 6 (2009) 252–268.
[32] M. Islam and R.K. Patel, Evaluation of removal efficiency of fluoride from aqueous solution using quick lime, J. Hazard. Mater., 143 (2007) 303–310.
[33] N. Das, P. Pattanaic and R. Das, Defluoridation of drinking water using activated titanium rich bauxite, J. Colloid. Interf. Sci., 292 (2005) 1–10.
[34] M. Yurdakoc, Y. Seki, S. Karahan and K. Yuedakoc, Kinetic and thermodynamic studies of boron removal by Siral 5, Siral 40, and Siral 80, J. Colloid. Interf. Sci., 286 (2005) 440–446.
[35] W.J. Weber and J.C. Morris, Kinetics of adsorption of carbon from solution, Am. Soc. Civ. Eng., 89 (1963) 31–60.
[36] S. Meenakshi and N. Viswanathan, Identification of selective ion-exchange resin for fluoride sorption, J. Colloid. Interf. Sci., 308 (2007) 438–450.